

Published in final edited form as:

*J Am Chem Soc.* 2010 September 29; 132(38): 13170–13171. doi:10.1021/ja1061399.

## Connecting energy landscapes with experimental rates for aminoacyl-tRNA accommodation in the ribosome

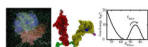
Paul C. Whitford, José N. Onuchic, and Karissa Y. Sanbonmatsu

Theoretical Biology and Biophysics, Theoretical Division, Los Alamos National Laboratory, MS K710, Los Alamos, NM, 87545.

Center for Theoretical Biological Physics and Department of Physics, University of California, San Diego, 9500 Gilman Dr, La Jolla, CA, 92093.

Paul C. Whitford: whitford@lanl.gov

### Abstract



Using explicit-solvent simulations of the 70S ribosome, the barrier-crossing attempt frequency was calculated for aminoacyl-tRNA elbow-accommodation. In seven individual trajectories (200–300 ns, each), the relaxation time of tRNA structural fluctuations was determined to be  $\sim 10$  ns and the barrier-crossing attempt-frequency of tRNA accommodation is  $\sim 1\text{--}10 \mu\text{s}^{-1}$ . These calculations provide a quantitative relationship between the free-energy barrier and experimentally-measured rates of accommodation, which demonstrate that the free-energy barrier of elbow-accommodation is less than  $15 k_B T$ , *in vitro* and *in vivo*.

Using explicit-solvent simulations of the 70S ribosome (3.2 million atoms for an aggregate 2.1  $\mu\text{s}$ . Table 1), we provide a quantitative relationship between free-energy profiles and experimentally determined kinetics for aminoacyl-tRNA (aa-tRNA) accommodation in the ribosome during tRNA selection (Figure 1). After initial selection, where the incoming aa-tRNA associates with the messenger RNA (mRNA) on the ribosome,<sup>1</sup> accommodation displaces the encoded amino acid  $\sim 90 \text{ \AA}$  from outside of the ribosome to the peptidyltransferase center (PTC), where it is added into the nascent protein chain. When near-cognate aa-tRNA molecules successfully associate during initial selection, accommodation acts as a “kinetic proofreading” step,<sup>2</sup> where incorrect tRNAs are often rejected by the ribosome. This kinetic process is governed by the underlying thermodynamics, which have been the focus of experimental<sup>3,4</sup> and theoretical<sup>5,6</sup> investigations.

Simulations and theoretical models have the potential to provide a structural/energetic framework for interpreting rapid kinetic and single-molecule measurements, though comparison is rarely direct. Specifically, kinetics are measured in bulk experiments, while free-energy profiles are far more difficult to obtain.<sup>7</sup> In contrast, many molecular simulation methods are available to calculate the potential of mean force (i.e. the free energy along a specific degree of freedom) for biomolecular processes,<sup>8</sup> while it is not feasible to directly measure rates. Consequently, calculations often focus on the fluctuations about particular configurations.<sup>9</sup>

Supporting Information Available: Simulation details. Description of rate calculations. This information is available free of charge via the Internet at <http://pubs.acs.org>

To connect experimental accommodation kinetics and the free-energy profile, one may use the relationship<sup>10</sup>

$$\frac{1}{k_a} = \langle \tau_a \rangle = \int_{Q_{A/T}}^{Q_{A/A}} dQ \int_{-\infty}^Q dQ' \frac{\exp[(G(Q) - G(Q'))/k_B T]}{D(Q)} \quad [1]$$

where  $k_a$  is the rate of accommodation,<sup>1</sup>  $\langle \tau_a \rangle$  is the mean-first passage time,  $Q$  is the reaction coordinate,  $G(Q)$  is the Gibbs free-energy,  $D(Q)$  is the diffusion in  $Q$ -space and  $Q_{A/T}$  and  $Q_{A/A}$  are the values of  $Q$  that define the A/T and A/A configurations (SI). If  $G(Q)$  has a single barrier, and  $D(Q)$  is constant (see SI), Equation 1 is approximated as

$$\frac{1}{k_a} \approx \frac{1}{C_a} \exp(\Delta G_{TSE}/k_B T) \quad [2]$$

where  $\Delta G_{TSE}$  is the difference in the free-energy of the A/T ensemble and the transition state ensemble (TSE).  $C_a$  is the barrier-crossing attempt frequency. While this general relationship relates kinetic rates and the free-energy profile, the attempt frequency  $C_a$  is process-specific. The barrier-crossing attempt frequency is determined by the diffusion and the distance between the endpoints (both in  $Q$ -space).

While accommodation is likely a multistep process,<sup>6</sup> here the discussion is restricted to tRNA-elbow accommodation (measured by  $R_{Elbow}$ ; Fig. 1), for comparison to single-molecule data.<sup>6,11</sup> To determine the attempt frequency, we calculated  $D_{Elbow}(R_{Elbow})$  (diffusion coefficient in  $R_{Elbow}$ ) from explicit-solvent simulations, set Equations 1 and 2 equal to each other and numerically integrated Equation 1. Since free-energy profiles of accommodation have not previously been determined, the functional form of  $G(R_{Elbow})$  was varied to establish robustness of the results (SI).

Simulations of the 70S ribosome, fully-solvated with physiological concentrations of ions, were performed (Table 1). The diffusion coefficient in elbow distance,  $D_{Elbow}$ , was determined using 2 different strategies. The first approach was to use the quasi-harmonic approximation to the dynamics, as employed in protein folding studies,<sup>12</sup> where

$D_{Elbow} = \langle \Delta R_{Elbow}^2 \rangle / (2\tau_{Elbow})$ .  $\langle \Delta R_{Elbow}^2 \rangle$  is the mean-squared fluctuations in distance and  $\tau_{Elbow}$  is the decay time associated with the fluctuations (Figures 2C–E). With this procedure,  $D_{Elbow}$  (labeled  $D_1$  in Table 1) for the A/T and A/A ensembles (SI) was  $1.1 \pm 0.1 \mu\text{m}^2/\text{s}$  and  $0.8 \pm$

$0.1 \mu\text{m}^2/\text{s}$ . The second strategy employed<sup>13</sup>:  $D_{Elbow} = \lim_{t \rightarrow \infty} \frac{\partial}{\partial t} \langle |R_{Elbow}(t) - R_{Elbow}(0)|^2 \rangle / 2$  The mean-squared displacement is linear from 10 and 20 ns, yielding diffusion coefficients (labeled  $D_2$  in Table 1) of  $0.8 \pm 0.2 \mu\text{m}^2/\text{s}$  (A/T) and  $0.5 \pm 0.2 \mu\text{m}^2/\text{s}$  (A/A). In the case of infinite sampling, the two approaches should yield identical values. Here, the two values of  $D_{Elbow}$  are within the statistical uncertainty. In solution, the diffusion coefficient of ternary complex has been estimated at  $0.3\text{--}2.5 \mu\text{m}^2/\text{s}$ .<sup>14</sup> Since diffusion is determined by the degree of roughness in the landscape, the striking similarity between the diffusion in solution and inside the ribosome suggests there is a low degree of roughness in the energy landscape of accommodation.

Figure 2F shows the accommodation rate  $k_a$  as a function of barrier height, obtained through numerical integration of equation 1 (SI), with  $D_{Elbow} = 1.1 \mu\text{m}^2/\text{s}$ . The attempt frequency  $C_a$  was also calculated as a function of barrier height. The attempt frequency is proportional to

<sup>1</sup>Referred to as  $k_5$  elsewhere.<sup>1</sup>

the curvature of the initial and final basins.<sup>15</sup> Since the curvature of the basins increases with increasing barrier height (see SI), the observed increase in attempt frequency (Figure 2F) is expected.

Depending on the barrier height and functional form (SI), the attempt frequency for elbow-accommodation is  $\sim 1\text{--}8 \mu\text{s}^{-1}$ , which is in the same range of values as for small RNA ( $0.1\text{--}1.6 \mu\text{s}^{-1}$ )<sup>16</sup> and protein ( $0.1\text{--}20 \mu\text{s}^{-1}$ )<sup>15</sup> folding.

Here, we employed  $D_{Elbow}=1.1 \mu\text{m}^2/\text{s}$ , which is our upper-bound estimate. Accordingly, the rate for a given barrier height, and the barrier height for a given rate, should be considered upper bounds. Bulk kinetic experiments have reported the rate of full accommodation to range from 10s to 100s per second<sup>3,4</sup> (Shaded blue in Fig 2F). These rates suggest barrier heights of  $\sim 9\text{--}13 k_B T$ .<sup>2</sup> Since accommodation is not barrier-less, targeting its TSE<sup>6,11</sup> is a viable approach for gaining quantitative control of translation. Finally, this study establishes the conversion between kinetics and free-energy profiles. With this conversion, it is now possible to validate the details of the free-energy profiles obtained from smFRET and simulations through comparison with kinetic data for large-scale conformational rearrangements in the ribosome.

## Supplementary Material

Refer to Web version on PubMed Central for supplementary material.

## Acknowledgments

This work was supported by the LANL LDRD program, NIH Grant R01-GM072686, the Center for Theoretical Biological Physics, sponsored by the NSF (Grant PHY-0822283), with additional support from NSF-MCB-0543906. We are also grateful for computing time on the NMCAC Encanto Supercomputer and the LANL Roadrunner Supercomputer.

## References

1. Rodnina MV, Wintermeyer W. *Annu Rev Biochem.* 2001; 70:415–435. [PubMed: 11395413]
2. Hopfield JJ. *Proc. Nat. Acad. Sci. USA.* 1974; 71:4135–4139. [PubMed: 4530290]
3. Gromadski KB, Rodnina MV. *Mol Cell.* 2004; 13:191–200. [PubMed: 14759365]
4. Johansson M, Bouakaz E, Lovmar M, Ehrenberg M. *Mol Cell.* 2008; 30:589–598. [PubMed: 18538657]
5. Sanbonmatsu KY, Joseph S, Tung C-S. *Proc. Nat. Acad. Sci. USA.* 2005; 102:15854–15859. [PubMed: 16249344]
6. Whitford PC, Geggier P, Altman R, Blanchard SC, Onuchic JN, Sanbonmatsu KY. *RNA.* 2010; 16:1196–1204. [PubMed: 20427512]
7. Schuler B, Lipman EA, Eaton WA. *Nature.* 2002; 419:743–747. [PubMed: 12384704]
8. (a) Garcia AE, Paschek D. J. *Amer. Chem. Soc.* 2008; 130:815–817. [PubMed: 18154332] (b) Vaiana A, Sanbonmatsu KY. *J. Mol. Biol.* 2009; 386:648–661. [PubMed: 19146858] (c) McDowell SE, Špačková N, Šponer J, Walter NG. *Biopolymers.* 2007; 85:169–184. [PubMed: 17080418] (d) Hansson T, Oosenbrink C, van Gunsteren WF. *Curr. Opin. Struct. Biol.* 2002; 12:190–196. [PubMed: 11959496]
9. (a) Besseová I, Réblová K, Leontis NB, Šponer J. *Nuc. Acid Res.* 2010 doi:10.1093/nar/gkq414. (b) Romanowska J, Setny P, Trylska J. *J. Phys. Chem. B.* 2008; 112:15227–15243. [PubMed: 18973356] (c) Trabuco LG, Harrison CB, Schreiner E, Schulten K. *Structure.* 2010; 18:627–637. [PubMed: 20462496] (d) Petrone PM, Snow CD, Lucent D, Pande VS. *Proc. Nat. Acad. Sci. USA.*

<sup>2</sup>This assumes elbow accommodation is rate limiting during accommodation.

- 2008; 105:16549–16554. [PubMed: 18946046] (e) Tama F, Valle M, Frank J, Brooks CL. Proc. Nat. Acad. Sci. USA. 2003; 100:9319–9323. [PubMed: 12878726]
10. (a) Bryngelson JD, Wolynes PG. J. Phys. Chem. 1989; 93:6902–6915. (b) Zwanzig R. Proc. Natl. Acad. Sci. USA. 1988; 85:2029. [PubMed: 3353365]
11. (a) Marshall RA, Aitken CE, Dorywalska M, Puglisi JD. Annu. Rev. Biochem. 2008; 77:177–203. [PubMed: 18518820] (b) Geggier P, Dave R, Feldman MB, Terry DS, Altman RB, Munro JB, Blanchard SC. J. Mol. Biol. 2010; 399:576–595. [PubMed: 20434456]
12. (a) Chahine J, Oliveira RJ, Leite VBP, Wang J. Proc. Nat. Acad. Sci. USA. 2007; 104:14646–14651. [PubMed: 17804812] (b) Socci ND, Onuchic JN, Wolynes PG. J Chem Phys. 1996; 104:5860–5868.
13. Yeh I-C, Hummer G. Biophys J. 2004; 86:681–889. [PubMed: 14747307]
14. Zhang G, Fedyunin I, Miekley O, Valleriani A, Moura A, Ignatova Z. Nuc. Acid. Res. 2010:384778–384787.
15. (a) Kubelka J, Hofrichter J, Eaton WA. Curr. Opin. Struct. Biol. 2004; 14:76–78. [PubMed: 15102453] (b) Tang J, Kang S-G, Saven JG, Gai F. J Mol Biol. 2009; 389:90–102. [PubMed: 19361525]
16. Thirumalai D, Hyeon C. Biochem. 2005; 13:4957–4970. [PubMed: 15794634]

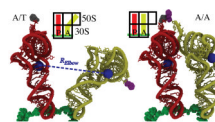


**Figure 1.** Structural representation of the aa-tRNA (yellow), p-tRNA (red), mRNA (green), and the associated amino-acids (grey, purple), in the partially-bound A/T conformation (left) and fully-bound A/A conformation (right). Elbow-accommodation is measured by  $R_{Elbow}$ : the distance between the O3' atoms of U8 on p-tRNA and U47 on aa-tRNA (blue spheres).

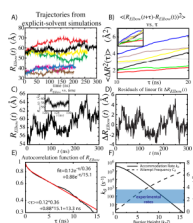


**Figure 2.**

A) Time traces of  $R_{elbow}$  from 7 explicit-solvent simulations. B) Mean-squared displacement  $\langle \Delta R_{elbow}^2(\tau) \rangle$  as a function of time delay  $\tau$ .  $D_{Elbow}$  was estimated by the slope between 10 and 20 ns. Inset shows  $\langle \Delta R_{elbow}^2(\tau) \rangle$  for  $\tau=0-30$  ns. C) 300 ns trajectory, displayed at 1 ns intervals. Inset shows subset at 5 ps intervals. D) Dispersion and relaxations were calculated from the residuals of linear fit (slopes in Table 1),  $\Delta R_{elbow}$ . E) Autocorrelation function of  $\Delta R_{elbow}$  fitted to sum of 2 exponentials (SI).  $D_{Elbow}$  was calculated from the average decay time  $\langle \tau \rangle$ . F) Accommodation rate  $k_a$  and attempt frequency  $C_a$ , for  $D_{Elbow}=1.1\mu\text{s}^2/\text{s}$ , versus the free-energy barrier height. Range of experimentally-determined rates shaded in blue.

Table 1

Summary of diffusion coefficient calculations.

conf	length (ns)	drift (Å/ns)	$\langle \Delta R^2 \rangle$ (Å <sup>2</sup> )	$\langle \tau \rangle$ (ns)	$D_I$ ( $\mu\text{m}^2/\text{s}$ )	$D_2$
A/T	301	$1.5 \times 10^{-2}$	3.27	13.3	1.2	1.1
A/T	262	$3.3 \times 10^{-2}$	5.79	35.4	0.8	0.9
A/T	260	$-3.0 \times 10^{-2}$	4.07	17.3	1.2	0.6
A/T	261	$4.5 \times 10^{-4}$	1.91	8.46	1.1	0.3
A/A	208	$1.1 \times 10^{-2}$	2.76	19.7	0.7	1.0
A/A	205	$9.4 \times 10^{-3}$	1.36	11.7	0.6	0.3
A/A	213	$2.7 \times 10^{-2}$	1.47	7.64	1.0	0.2